J/ψ at finite temperature - Lattice QCD result and potential model analysis

H. Matsufuru*, O. Miyamura†, H. Suganuma** and T. Umeda†

*Research Center for Nuclear Physics, Osaka University, Ibaraki 567-0047, Japan
(present address is YITP, Kyoto University, Kyoto 606-8502, Japan.)
†Department of Physics, Hiroshima University, Higashi-hiroshima 739-8526, Japan
**Faculty of Science, Tokyo Institute of Technology, Tokyo 152-8551, Japan

Abstract.
We study the charmonium correlators in the deconfined phase, as well as at $T < T_c$, in two viewpoints. One is an analysis of correlation between quark and antiquark in the finite temperature lattice QCD at the quenched level. The result implies that the correlation is so strong that the quark and antiquark still tend to stay together even at $T \simeq 1.5T_c$. On the other hand, the potential model analysis, the second approach, results in the existence of no bound state at $T \simeq 1.2T_c$. The static quark potential obtained in lattice simulation is used in the latter analysis. The change of the bound state energy below T_c is also studied.

INTRODUCTION

The change of J/ψ properties near the QCD phase transition is one of most important signals of the formation of quark gluon plasma [1, 2]. Compared with the recent development of the heavy-ion collision experiment [3], theoretical understanding of the charmonium at $T > 0$ is not yet sufficient and its progress is desired. Although the lattice QCD simulation at $T \neq 0$ may give a stage of such an investigation directly based on QCD, at present only exploratory studies have been done [4]. Phenomenological approaches are thus important to understand the nature of hadronic states at finite temperature, as well as at finite density, where the lattice QCD is hardly applicable.

The most important ingredient of the potential model approaches is the static quark-antiquark potential, and it is numerically derived from the lattice QCD as a reliable quantity. On the other hand, both the lattice QCD and the potential model can provide the hadron properties. In this way, there is a mutual connection between lattice QCD simulations and phenomenological potential model analysis, and the consistent understanding between them would be significant.

In this paper, we discuss the fate of the charmonium above the critical temperature T_c, from the following two points of view.

(i) Finite temperature lattice QCD.
The charmonium correlator in the deconfined phase is studied using the finite temperature lattice QCD. Here we focus on the change of the q-$\bar{q}$ spatial correlation in terms of the Euclidean time t [4]. In the deconfined phase, q-$\bar{q}$ spatial correlation is naively expected to broaden as t, from a simple picture of almost free quarks.

The static quark potential, which is an important ingredient of the potential model approach, is also measured [5].

(ii) Potential model analysis based on lattice QCD.
In the deconfined phase, the static quark potential is expected to be the Yukawa-type form characterized by its screening mass. This is indeed observed in the lattice QCD simulation [5, 6]. We employ the potential model approach together with the obtained static potential on the lattice for an investigation of the charmonium properties. First subject is the stationary state problem which give the condition of existence for a bound state. Below T_c, we observe the change of bound state energy accompanied by the change of the static quark potential as T. In the deconfined phase, we study whether the charmonium bound state is formed in the Yukawa potential. Then by solving the evolution of the wave function governed by the Schrödinger equation, we would estimate the decay distance of the created $c\bar{c}$ pair. (Even if the bound state is not formed, if the created $c\bar{c}$ pair keeps strong correlation during certain time period, $c\bar{c}$ pair may escape from the plasma phase without decaying and can form the charmonium state.)

The results of these two analyses are compared with each other. The present simulation is at the quenched level, which contains no dynamical quark effect. These results may give an important qualitative implications, and will be compared with the results on lattices with dynamical quark effect. At present, the last subject in (ii) is in progress, and we comment only on the technical point for a computation.

The next section describes the result of lattice QCD simulations, the charmonium correlator and the static Q-$\bar{Q}$ potential. In successive section, the potential model analysis is presented. The last section is devoted for summary and outlook.

LATTICE QCD RESULT

In this section, we summarize the results from lattice QCD simulations [4, 5].

Correlator analysis. Lattice QCD provides a nonperturbative procedure to investigate hadron correlators directly based on QCD. At finite temperature, however, an analysis of them must overcome several difficulties to obtain relevant result. One of them is a shortage of information in the temporal direction, since the temporal extent is restricted by the condition $T = 1/(N_t a_\tau)$, where a_τ is the temporal lattice spacing and N_t is the temporal lattice size. To increase N_t (therefore to decrease a_τ) keeping the spatial lattice size modest, we employ the anisotropic lattice [8]. Even on an anisotropic lattice, extraction of relevant information from the hadron correlators is a difficult task. QCD-TARO Collaboration measured the spatial q-$\bar{q}$ correlation and discussed their dependence on Euclidean time t to probe the possibility of the bound states [7]. This analysis has been applied also to the charmonium system [4], which we briefly summarize in the following.

The numerical simulation has been carried out on the lattices with sizes $16^2 \times 24 \times N_t$, at the quenched level. Gauge configurations have been generated with the anisotropic Symanzik (tree-level) action with parameters corresponding to the renor-

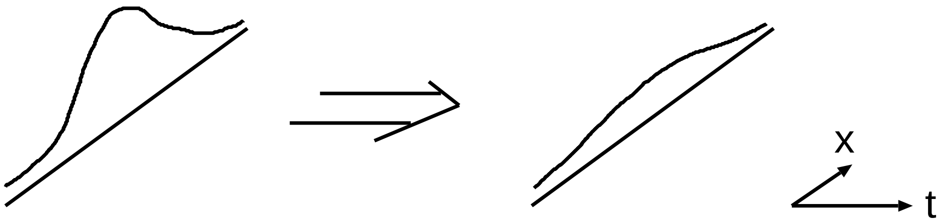

FIGURE 1. Schematic expected behavior of the q-$\bar{q}$ correlator without bound states.

malized anisotropy $\xi \equiv a_\sigma/a_\tau = 3.95(2)$ and the lattice cutoffs a_σ^{-1}=1.61(1) GeV ($a_\sigma \simeq 0.125$ fm) and a_τ^{-1}=6.36(5) GeV. Used N_t's are as follows: N_t =96 ($T \simeq 0$), 28 (0.87 T_c), 26 (0.93 T_c), 20 (1.22 T_c) (for static potential) and 16 (1.52 T_c) (for q-$\bar{q}$ correlator analysis). The configurations are fixed to the Coulomb gauge. As the quark action, we adopt the $O(a)$ improved Wilson action [4, 9]. The quark parameters are tuned roughly so as to correspond to the charm quark mass.

The spatial correlation between quark and antiquark is represented by

$$w_\Gamma(r,t) = \sum_{\vec{x}} \langle \bar{q}(\vec{x}+\vec{r},t)\Gamma q(\vec{x},t) O_\Gamma^\dagger(0)\rangle, \tag{1}$$

where 4×4 matrix Γ specifies the spin quantum number. We focus on the vector channel in the following. As the operator $O_\Gamma(x)$, which overlaps with the meson states, we use the form $O_\Gamma(x) = \sum_{\vec{y}} \bar{q}(\vec{x}+\vec{y},t)\varphi(\vec{y})\Gamma q(\vec{x},t)$. The smearing function $\varphi(\vec{y})$ is tuned so that the overlap with the ground state is exclusively large. We observe the t-dependence of this correlator. The idea is rather simple: if there is no bound state (like free quark case), this q-$\bar{q}$ correlator becomes broader as t (Euclidean time), as in Figure 1. In this case, the normalized correlator at the spatial origin,

$$\phi_\Gamma(r,t) = w_\Gamma(r,t)/w_\Gamma(r=0,t), \tag{2}$$

increases with t.

Figure 2 shows the q-$\bar{q}$ correlation in the simulation, together with the case of free quarks smeared with the same function as in the simulation. In the left figure, at $T < T_c$, the $\phi_\Gamma(r,t)$ approaches to a stable shape with t. In contrast, the correlator with free quark and antiquark becomes broader with t, as expected. In the right figure, at $T \simeq 1.5T_c$, the correlator shows essentially the same feature as below T_c. This is qualitatively different behavior from the free quark case. This implies that up to this temperature the quark and the antiquark keeps strong correlation so that they still stay together. Although what the q-$\bar{q}$ correlator strictly means is not obvious than at $T = 0$, this result suggests the possibility of persistence of the bound state even in the deconfined phase.

As the next step, we examine this question in the potential model analysis. Before going into this subject, we obtain here the static quark potential used in the potential model on the same series of lattices.

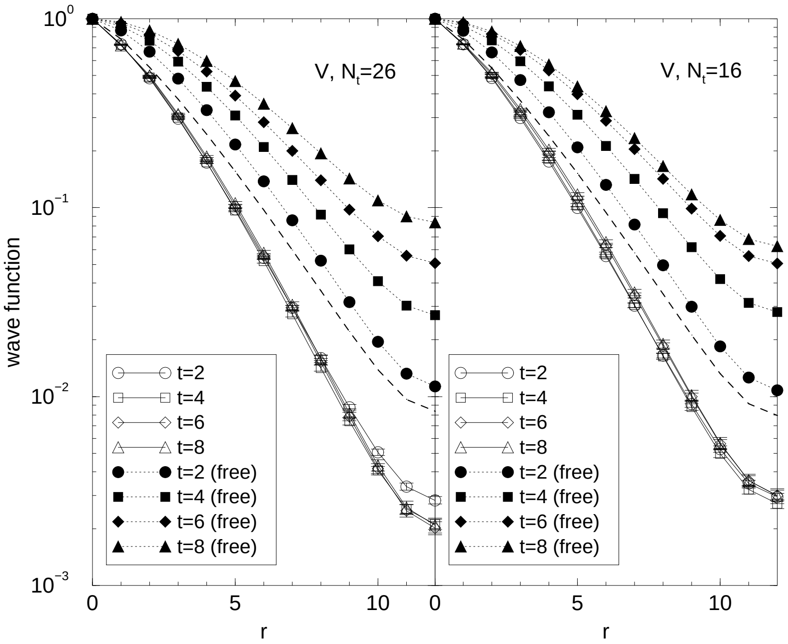

FIGURE 2. Observed q-$\bar{q}$ correlator, $\phi_\Gamma(r,t)$, below (left) and above (right) T_c. The dashed line is the smearing function.

Static quark potential. The static quark-antiquark potential at finite temperature is extracted from the correlation of the Polyakov loops,

$$P_2(\vec{r}) = \langle P(0)P^\dagger(\vec{r})\rangle \simeq c \cdot \exp(-V_{Q\bar{Q}}(\vec{r})N_\tau), \tag{3}$$

where $P(\vec{x})$ is the Polyakov loop,

$$P(\vec{x}) = \mathrm{Tr} \prod_{t=0}^{N_\tau-1} U_4(\vec{x},t). \tag{4}$$

We have measured the static quark potential on the same series of lattice used for the analysis of q-$\bar{q}$ spatial correlation.

The potentials at $T \neq 0$ are shown in Figure 3. Below T_c, we fit the obtained result to the form

$$V_{Q\bar{Q}}(r) = -\frac{A}{r} + \sigma r + C, \tag{5}$$

where the first term is the one-gluon-exchange Coulomb term, the second term is the confining linear term with the string tension σ, and the last term is constant due to the finiteness of lattice spacing. At $T = 0$, this form is known to well describe the potential obtained on the lattice. In Table 1, we summarize the result of fit at three values of T containing $T \simeq 0$. The large χ^2/N_{df} signals a large systematic error due to the lattice artifact for $T \simeq 0$. The values of the coefficient of the Coulomb term is not so reliable since the short range part is not appropriately incorporated in the fit. The string tension

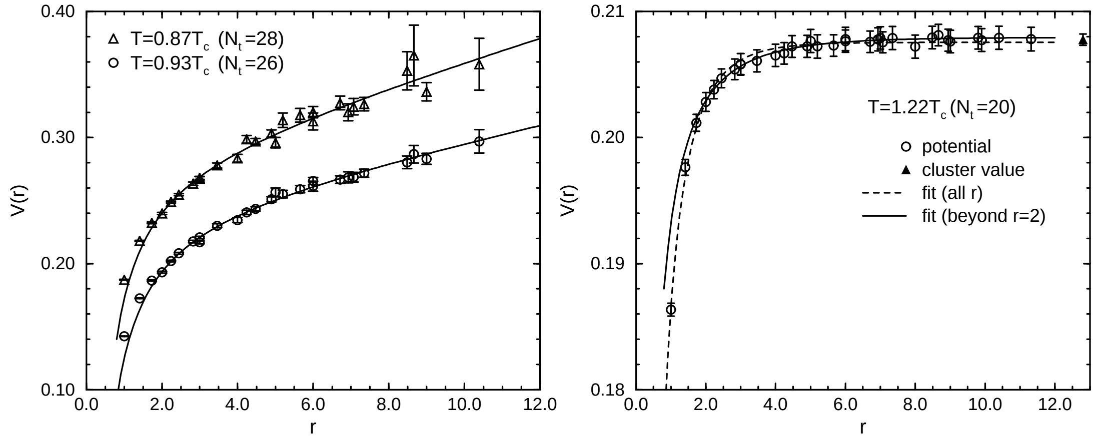

FIGURE 3. The lattice QCD results for the static quark potentials below (left) and above (right) T_c. In the left figure, upper data at $N_t = 28$ correspond to $T \simeq 0.87T_c$, and lower data at $N_t = 26$ correspond to $T \simeq 0.93T_c$. They are vertically slightly shifted. The solid lines are the fitted curves. In the right figure, the triangle symbol denotes the cluster value, which corresponds to the product of two independent Polyakov loops.

TABLE 1. Result of the fit for the potential below T_c. The last two columns are the same A and σ in the physical unit (the errors are omitted). A dimensionless quantity A is changed due to the anisotropy.

N_τ	T	fit range	A	σ	C	χ^2/N_{df}	$A_{(phys)}$	$\sigma_{(phys)}$
96	~ 0	$r \geq 2.8$	0.0587(49)	0.01781(29)	0.0587(49)	78.1/18	0.23	0.18 GeV^2
28	$0.87T_c$	$r \geq 2$	0.119 (11)	0.0089(11)	0.2817(70)	25.2/21	0.47	0.091 GeV^2
26	$0.93T_c$	$r \geq 2$	0.1253(63)	0.00638(7)	0.2934(41)	23.5/21	0.49	0.065 GeV^2

decreases with increasing T. In Table 1, we also quote the values of A and σ converted into the physical unit for the later use in the potential model analysis.

The right figure in Figure 3 shows the static potential above T_c ($T \simeq 1.2T_c$). In the deconfined phase, it is known that the potential is well described by the Yukawa-type form [6],

$$V_{Q\bar{Q}}(r) = -A\exp(-\mu r)/r + C, \tag{6}$$

with the screening length as $1/\mu$. The extracted value of μ strongly depends on the fit range, and results in about $0.5 \sim 1$ GeV. One of our goal is to examine whether the bound state can survive with this screened potential.

POTENTIAL MODEL APPROACH

Stationary state analysis. For the charmonium system, the nonrelativistic approximation is applicable [10]. The subject we are interested in is essentially the T-dependence of the binding energy and the condition in which the bound state dis-

TABLE 2. Result of fit for the potential at $T = 1.2T_c$. The last two columns are the same A and μ in the physical unit (the errors are omitted). A dimensionless quantity A is changed due to the anisotropy.

range	A	μ	C	χ^2 / N_{dof}	$A_{(phys)}$	$\mu_{(phys)}$
all r	0.0469(15)	0.803(40)	0.20755(88)	5.29 / 24	0.185	1.29 GeV
$r \geq 2$	0.0217(33)	0.385(73)	0.20794(87)	1.03 / 21	0.086	0.62 GeV

appears. In this work, therefore, we treat the Schrödinger equation for a spin averaged states. For the stationary state, the equation to be solved is

$$\left(-\frac{\Delta}{2m_R} + V(x)\right)\psi(x) = E\psi(x), \tag{7}$$

with the reduced mass, $m_R = m_Q/2$. For the S-state, this equation is reduced to

$$\left(-\frac{1}{2m_R}\frac{d^2}{dr^2} + V(r)\right)u(r) = Eu(r), \tag{8}$$

where $u(r) = r\psi_r(r)$ and $\psi_r(r)$ is the radial wave function. As the potential $V(r)$, we use the form in the previous section with parameters obtained in lattice QCD simulation.

Let us start with the change of the binding energy below T_c. As the potential $V(r)$, we use the form of eq. (5) without the constant term, which is due to the finite lattice spacing. The values of A and σ are set to ones determined in lattice QCD simulation (listed in the last two columns of Table 1). Eq. (8) is numerically solved and gives the binding energy as the function of m_Q as shown in the left figure of Figure 4. The binding energy with a fixed quark mass decreases as T approaches toward T_c. This is a natural tendency accompanied by the decrease of the string tension. Quantitatively, however, we may need the precise determination of the Coulomb coefficient A, because the charmonium state tends to have a small radius and then its precise spectroscopy requires the precise value of A. In fact, the present analysis of the static quark potential is to be developed with the accurate Coulomb coefficient A. With the quantitative determination of A, the potential model can provide the T-dependence of charmonium spectrum reflecting the T-dependence of the static potential based on QCD.

Above T_c, the potential is expressed with the screened form, eq. (6), without the constant term, which corresponds to the intrinsic energy concerning the static quark in the deconfined phase. In this case, we solve eq. (8) for fixed A and m_Q and obtain the binding energy as a function of μ. The right figure of Figure 4 shows the result for $A = 0.086$ and $m_Q = 1.3$GeV. Around $\mu \simeq 0.065\text{GeV} \equiv \mu_c$, the binding energy vanishes, and no bound state is formed for larger value of $\mu > \mu_c$. On the other hand, from Table 2, the value of μ at $T \simeq 1.2T_c$ is about 0.62 GeV, which is sufficiently larger than the critical value μ_c at which the bound state disappears. Similar result is also obtained for the case of $A = 0.185$. Therefore, we conclude that there exists no bound state at $T \simeq 1.2T_c$ from the analysis with the Q-$\bar{Q}$ potential obtained in quenched lattice QCD. This is a reproduction of the result by Karsch, Mehr and Satz [11]. On the lattice with dynamical configuration, the screening effect may be stronger, and this conclusion would not to be changed.

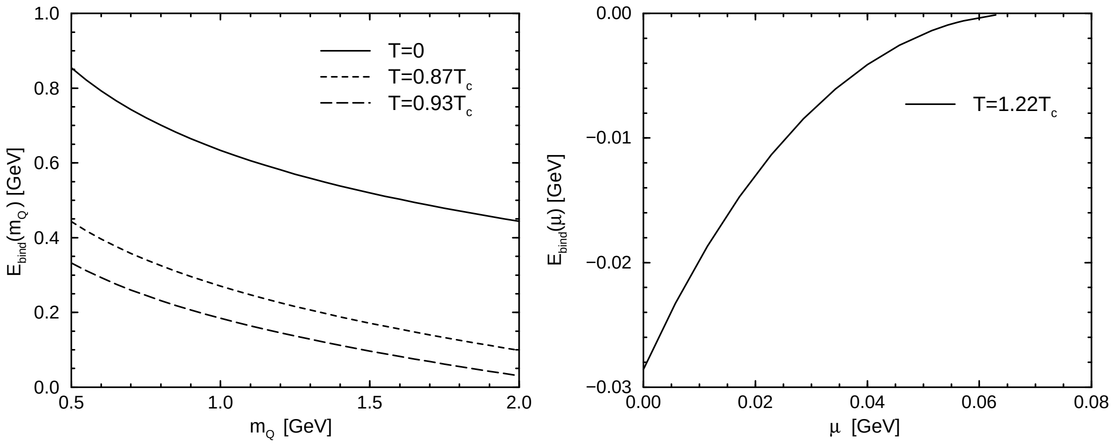

FIGURE 4. The potential model results for the binding energy below (left) and above (right) T_c. The left figure shows the binding energy as the function of m_Q at three values of T. The right figure shows the binding energy at $T > T_c$ as the function of μ. Here, $A = 0.086$ and $m_Q = 1.3$ GeV are used.

This result seems contradicting our previous result for q-$\bar{q}$ correlation at $T \simeq 1.5T_c$. In the latter case, the genuine dynamics of time evolution is not incorporated, and the argument concerning the bound state is based on a sort of conjecture. Since the temporal lattice extent is restricted to $1/T$, the dynamics of time scale larger than $1/T \sim 1$ fm is not probed. Then the next question is what is the time scale after which the quark and antiquark are well separated. To answer this question, in the scope of the potential model, we treat the time evolution problem of the Schrödinger equation.

Toward non-stationary state analysis. To analyze the time evolution of the quark-antiquark system in the potential model, one needs to treat the time-dependent Schrödinger equation

$$i\frac{\partial}{\partial t}\psi(x) = \left(-\frac{\Delta}{2m_R} + V(x)\right)\psi(x). \tag{9}$$

With the Coulomb-like potential, one needs to manage the singularity in the vicinity of the spatial origin in the practical numerical computation. The most appropriate coordinate system is the modified cylindrical coordinate [12],

$$x = \xi^{2/3}\cos\phi, \qquad y = \xi^{2/3}\sin\phi, \qquad z = z. \tag{10}$$

The investigation based on this framework is now in progress, and would give an insight on the above-mentioned problem.

SUMMARY AND OUTLOOK

In this work, we have studied the properties of charmonium state in the lattice QCD and the potential model with the static potential measured in the lattice QCD.

In the lattice simulation, we have measured the q-$\bar{q}$ correlation in the deconfined phase as well as at $T < T_c$, and have found that the correlation is so strong that the quark and antiquark still stay together even at $T \simeq 1.5T_c$. The q-$\bar{q}$ correlator shows qualitatively different behavior from the free quark case, which may suggest the possibility of existence of the bound state even above T_c. The static quark potential is also measured on the same series of lattice. Another possible procedure to clarify the nature of hadronic correlators at $T > 0$ is the direct extraction of the spectral function [13].

In the potential model analysis for the stationary state, we have found contradicting result on the problem of the bound state in the deconfined phase: the bound state is not formed for the Yukawa-type static potential obtained in the lattice QCD at $T \simeq 1.2T_c$. To understand these two results, we are now preparing for the potential model analysis of non-stationary state problem. The change of the binding energy of the charmonium state below T_c is also an important result, and more quantitative analysis is desired.

Although present lattice calculation is at the quenched level, i.e. without dynamical quark effect, these analyses would give us an insight on the temperature effect on the charmonium state. The similar investigation on the charmonium at $T \neq 0$ is easily applicable to the simulation with dynamical quarks, in principle, and is expected to provide a novel information on the signal of quark-gluon-plasma formation.

We would like to thank to Profs. Il-Tong Cheon and Su Houng Lee for their warm hospitality at Yonsei University. The numerical simulation has been done on Intel Paragon XP/S and NEC HSP at INSAM, Hiroshima University and NEC SX-4 at Osaka University. H.M. is supported by center-of-excellence (COE) program at RCNP, Osaka University.

REFERENCES

1. T. Hashimoto, O. Miyamura, K. Hirose and T. Kanki, Phys. Rev. Lett. **57**, 2123 (1986).
2. T. Matsui and H. Satz, Phys. Lett. B **178**, 416 (1986).
3. NA50 Collaboration, Phys. Lett. B **477**, 28 (2000).
4. T. Umeda, R. Katayama, O. Miyamura and H. Matsufuru, hep-lat/0011085, to appear in Int. J. Mod. Phys. A.
5. H. Matsufuru, Y. Nemoto, H. Suganuma, T.T. Takahashi and T. Umeda, Nucl. Phys. B (Proc. Suppl.) **94**, 554 (2001).
6. M. Gao, Phys. Rev. D **41**, 626 (1990).
7. QCD-TARO Collaboration (Ph. de Forcrand et al.), Phys. Rev. D **63**, 054501 (2001).
8. F. Karsch, Nucl. Phys. **B205**, 285 (1982).
9. J. Harada, A.S. Kronfeld, H. Matsufuru, N. Nakajima and T. Onogi, hep-lat/0103026.
10. E. Eichten, K. Gottfried, T. Kinoshita, K.D. Lane and T.-M. Yan, Phys. Rev. D **17**, 3090 (1978), D **21**, 313 (1980) (E), D **21**, 203 (1980).
11. F. Karsch, M.T. Mehr and H. Satz, Z. Phys. C **37**, 617 (1988).
12. H. Kono, A. Kita, Y. Ohtsuki and Y. Fujimura, J. Comput. Phys. **130**, 148 (1997).
13. Y. Nakahara, M. Asakawa and T. Hatsuda, Phys. Rev. D **60**, 091503 (1999).